

Numerical Methods in Civil Engineering

Journal Homepage: <https://nmce.kntu.ac.ir/>

Numerical Simulation of Engineered Material Arrestor System (EMAS)

Amirhossein Akbarikermani*, Farzin Kalantary*

ARTICLE INFO

RESEARCH PAPER

Article history:

Received:

November 2020

Revised:

October 2024

Accepted:

December 2024

Keywords:

Aircraft;

Engineered Materials

Arrestor System (EMAS);

Numerical simulation;

Finite Element;

Arbitrary Lagrangian-

Eulerian

Abstract:

With the increasing speed and weight of modern passenger aircraft, the need for longer runways has become more critical than ever. To address safety concerns, the Federal Aviation Administration (FAA) has mandated a 305-meter (1,000-foot) safety zone, known as the Runway Safety Area (RSA), at the end of runways at major airports. However, in many cases, this requirement cannot be met due to natural or man-made obstacles within the airport's boundaries. As a solution, the implementation of an Engineered Material Arrestor System (EMAS) has been proposed. EMAS is designed to significantly reduce the stopping distance of aircraft during overrun events, minimizing both passenger discomfort and the risk of structural damage to the aircraft. The objective of this paper is to investigate and simulate the performance of EMAS using finite element analysis software capable of handling large deformation problems. The Arbitrary Lagrangian-Eulerian (ALE) formulation is utilized to conduct large deformation analyses. In the simulations, three types of aircraft are modeled to enter a hypothetical EMAS bed at a speed of 70 knots (130 km/h). Additionally, three types of foam concrete with different densities are selected for the EMAS bed material. The results demonstrate that higher-density materials exhibit greater stiffness, resulting in shorter stopping distances for the aircraft. As expected, lower-density (softer) materials apply less force and deceleration to the aircraft. Furthermore, the findings indicate that lighter aircraft experience higher deceleration forces than heavier aircraft, regardless of the bed material. However, heavier aircraft generate higher overall impact forces during the overrun.

1. Introduction

Between 1978 and 1987, the Federal Aviation Administration (FAA) reviewed accidents and incidents related to the takeoff and landing of US passenger aircraft and categorized 246 accidents as follows: undershooting (18), landing off the runway (11), veer-offs (97), overruns (33), or other (87). Events in which aircraft-ground impact occurred 2000 ft (610 m) or more from the runway, or where the aircraft experienced ground impact after becoming airborne during takeoff, were categorized as "Other" [1]. Between 1980 and 1998, 180 aircraft overrun accidents and incidents occurred in the English-speaking world [2]. Hall et al. (2008) compiled a database from available data of 459 overrun accidents and incidents that almost entirely occurred between 1982 and 2006 [3]. Many similar accidents also occurred in Iran, the most recent of which involved the

landing of a Caspian McDonnell Douglas MD-83 aircraft at Mahshahr Airport.

The plane landed 170 meters from the end of the runway on the Mahshahr-Sarband highway.

To reduce overrun incident hazards, the Federal Aviation Administration (FAA) requires a 305 m (1,000 ft) runway safety area beyond the runway end [4]. However, many airports are unable to construct this runway safety area due to natural or man-made barriers. In such cases, the FAA provides airport operators with the alternative of installing an Engineered Materials Arrestor System (EMAS).

Numerous studies have been conducted on EMAS. For example, Angley et al. (2004) conducted experiments on phenolic foam, and the results showed the system's ability to stop aircraft [5]. Barsotti et al. (2009), following a full-scale experiment, found that the rebound of cellular cement mortars was negligible under wheel loads. Nevertheless, some problems remained due to undesired pulverization and the low durability of the cement used in EMAS [6]. In 2010, Santagata et al. conducted experiments on cement mortars with high air content and expanded polystyrene analyses

* Department of Civil Engineering, K.N. Toosi University of Technology, Tehran, Iran

Corresponding author. E-mail address: a.akbarikermani@gmail.com.

under the action of the wheel of EMAS, providing effective theoretical support for further research on the EMAS of aircraft pavement [7]. Heymsfield et al. (2007) conducted a sensitivity analysis to identify key design parameters for engineered materials arresting systems (EMAS), providing a foundation for their optimization [8]. In 2008, Heymsfield expanded his research by exploring low-density concrete mixes to improve soft ground arrestor systems [9]. In 2013, he developed predictive models to estimate aircraft stopping distances, considering factors like aircraft type and arrestor material properties [10]. Zhang et al. (2013) created a MATLAB-based analytical model to study the impact of critical parameters, such as aircraft weight, material properties, and arrestor configuration, on foamed concrete arrestor system design [11]. Zhao (2014) performed static and dynamic analyses to evaluate the interaction between aircraft wheels and EMAS, offering theoretical insights to improve foamed concrete arrestor systems for aircraft pavements [12]. To evaluate the performance of the foamed concrete arrestor system, Zhang et al. (2015) performed a full-scale arresting test with an instrumented Boeing 737-300 aircraft. They then examined the validity of the analytical prediction model developed in the previous study using the full-scale test data [13]. Xing et al. (2017) studied the arresting properties of metal honeycomb material and proposed a Tire-Honeycomb Material Interaction Mechanical Model. By combining the dynamic model of the aircraft, they coded the theoretical model using MATLAB to complete the arresting simulation on aircraft B737-900ER and B727-100. In addition, a finite element model of the tire-honeycomb material interaction was built to verify the correctness of the theoretical model. In comparison with the results of traditional materials, the calculated results showed that the honeycomb material can stop the overrunning of the aircraft more efficiently while ensuring that the forces induced by the stopping process are safe for the passengers and aircraft. Yang et al. (2018) introduced the concept, structural construction, standard EMAS, installation, and maintenance of EMAS and reviewed the analytical modeling methods, finite element simulation techniques, full-scale arresting experimental approaches, and risk models, respectively [14].

In this study, the performance of EMAS is investigated using numerical modeling. Finally, the outputs related to stopping distance, deceleration, and reaction force on the wheel are presented in diagrams.

2. Engineered Materials Arrestor System (EMAS)

EMAS is an acceptable solution to reduce the risk of overrunning. Engineered materials are defined by the FAA as high-energy-absorbing materials of selected strength. As

an aircraft enters the EMAS, it creates a gradual transition from the paved ramp into a highly crushable bed. The aircraft wheels–runway surfacing interface exceeds the strength of the EMAS blocks, creating a resistive load that quickly decelerates and ultimately stops the aircraft [15], [16]. An example of the performance of this system is shown in Figure 1.

EMAS dimensions can vary considerably, but typical dimensions are approximately 300 ft in length by 150 ft in width, with a nominal 75-ft setback from the runway end. The design parameters for an EMAS are based on FAA requirements contained in Advisory Circular 150/5220-22A. This advisory circular requires that an EMAS have a standard design exit speed of 70 knots (standard case) and a minimum of 40 knots (non-standard case) [6].



Fig. 1: McDonnell Douglas MD-11 runway overrun, John F. Kennedy International Airport, New York, 2003 [17].

3. Numerical modeling

This study aims to investigate and simulate EMAS using finite element software (i.e., ABAQUS), which can simulate large deformation problems. The Arbitrary Lagrangian-Eulerian (ALE) formulation is used for large deformation analyses. Three planes are intended to arrive at a hypothetical bed at a speed of 70 knots. Three types of foam concrete with different densities were selected for the bed.

3.1 Arbitrary Lagrangian-Eulerian (ALE) Finite Element Formulations

In similar research, the Smoothed Particle Hydrodynamics (SPH) method is recommended for modeling the performance of the engineered material arresting system. In mesh-free formulations like SPH, as node connections are not used, mesh distortion and its problems do not occur. Therefore, particles are allowed to move freely. In addition, particle interactions are determined through calculations. This characterization of non-specified meshed particles makes free-mesh methods extremely computationally efficient [14], [18].

The Arbitrary Lagrangian-Eulerian (ALE) method is an explicit numerical formulation that has become a standard tool for solving large deformation problems in solid mechanics [19]. The initial description of the ALE methodology by Hirt et al. (1974) [20] is a remarkable paper in the literature. The ALE method combines the best features of the Lagrangian and Eulerian methods to provide a complete algorithm. The ALE method, along with a supplementary set of equations in terms of material and mesh displacements, is established through a mesh motion scheme, and then the two sets of unknown displacements are solved simultaneously [19], [21].

Subsequently, this method is validated by the pendulum test, and its results are adequately in harmony with experiments.

3.2 Validation of ALE method for pendulum test

The pendulum test apparatus featured a heavy 4,400-lb mass that hung from an overhead support frame, allowing it to swing in an arc of 24.5 ft. The mass was hoisted to the desired height and then released; the speed of the mass was controlled by the release height (Figure 2).

An example of this experiment was conducted by Barsotti et al. (2009). To reduce the number of variables in the design, a rigid aluminum wheel form was used instead of a pneumatic tire. The diameter and width were 14.8 in. and 5.5 in., respectively. Below the pendulum assembly, a box was constructed to retain larger blocks of glass foam. The overall dimensions were 9 ft in length, 2 ft in width, and 10 in. in height [6].



Fig. 2: Overview of pendulum test for glass foam [6].

2D numerical modeling (Figure 3) is performed according to the specifications of the Barsotti et al. (2009) experiment. The pendulum penetrates the bed by 4 inches, and its speed is set at 24.8 ft/s. The modeling of the wheel is done using a rigid element, and the friction coefficient between the wheel and the bed is assumed to be 0.25. The Tresca model is used

to simulate the materials. Poisson's ratio, modulus of elasticity, yield stress, and density are considered to be 0, 2000 psi, 155 psi, and 6 pcf, respectively. To create the initial boundary conditions, the displacement in the lower boundary is considered to be zero. It should be noted that the wheel only has a transient motion. Also, the ALE technique has been used for the middle region due to wheel penetration and mesh distortion.

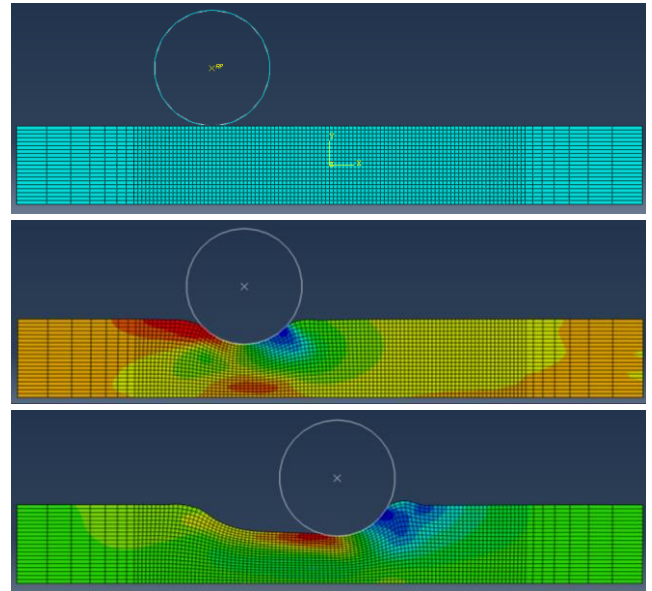


Fig. 3: 2D numerical modeling for pendulum test.

3.3 Modeling details of aircraft and foamed concretes

The EMAS system is simulated in two-dimensional form (Figure 4). Aircraft tires are considered rigid. Tire entry speed and EMAS length are assumed to be 70 knots and 300 meters, respectively. The friction coefficient of the tire and the arrester bed is assumed to be 0.25. The arrester bed consists of four rows of 48 cm high EMAS blocks that are seamlessly modeled. According to the Federal Aviation Administration [4], the maximum takeoff weight was used in the simulation. It should be noted that when the aircraft reaches a speed of about 2 m/s, the operation stops, and the system succeeds in stopping the aircraft.

Three planes are used for modeling: the DC-9-41 (relatively small in weight and size), the B727-100 (medium), and the B707-320C (relatively large). An exit speed of 70 knots, equal to 36 m/s, is assumed on a hypothetical bed of EMAS. The details of the aircraft are shown in Table 1.



Fig. 4: 2D model of EMAS for three aircraft.

Table 1: The details of the aircraft [22].

	Aircraft type		
	DC-9-41	B727-100	B707-320C
maximum takeoff weight (kg)	51700	76700	151500
maximum landing weight (kg)	46300	64700	112100
Moment of inertia (kg×m ²)	2440000	7100000	9570000
tire radius (m)	0.521	0.620	0.575
tire width (m)	0.381	0.439	0.406

In this study, three foamed concrete FC1, FC2, and FC3 with Different properties are investigated. Their properties are listed in Table 2.

Table 2: The details of foamed concrete FC1, FC2, and FC3 [11].

	ρ_0 (kg / m ³)	σ_y (MPa)	E(MPa)	ν
FC1	274.6	0.29	9.6	0
FC2	302.4	0.35	14.5	0
FC3	337	0.43	21.3	0

4. Analysis results

4.1. Validation results

After modeling the pendulum test, the analysis is performed on it. Finally, the loads on the pendulum wheel were compared with the experimental results (Figures 5 and 6). As can be seen, the numerical results are in good agreement with the experimental results. Although there is no 100% compliance, the overall trend of drag and vertical force changes over time is in good agreement. Therefore, the Tresca model and the ALE method are acceptable options for modeling the arrestor system.

4.2. Performance of three aircraft on different arrestor bed

In this simulation, the bed with constant thickness is considered. The results are presented in Figures 7 to 10.

As can be seen, the highest displacement is for the B707-320C and the lowest for the DC-9-41. The higher-density foamed concrete has a higher hardness, which results in shorter stopping distances. As expected, the lower-density material causes less force on the aircraft and less acceleration. It should also be noted that the drag force depends on the weight of the aircraft.

At the end of the force-displacement and acceleration-displacement diagrams, there are jumps in values due to a sudden decrease in velocity at the end of the stopping distance. It is expected that if the wheel is simulated as flexible, the diagrams will be slightly smoothed and the stopping distance will be shorter.

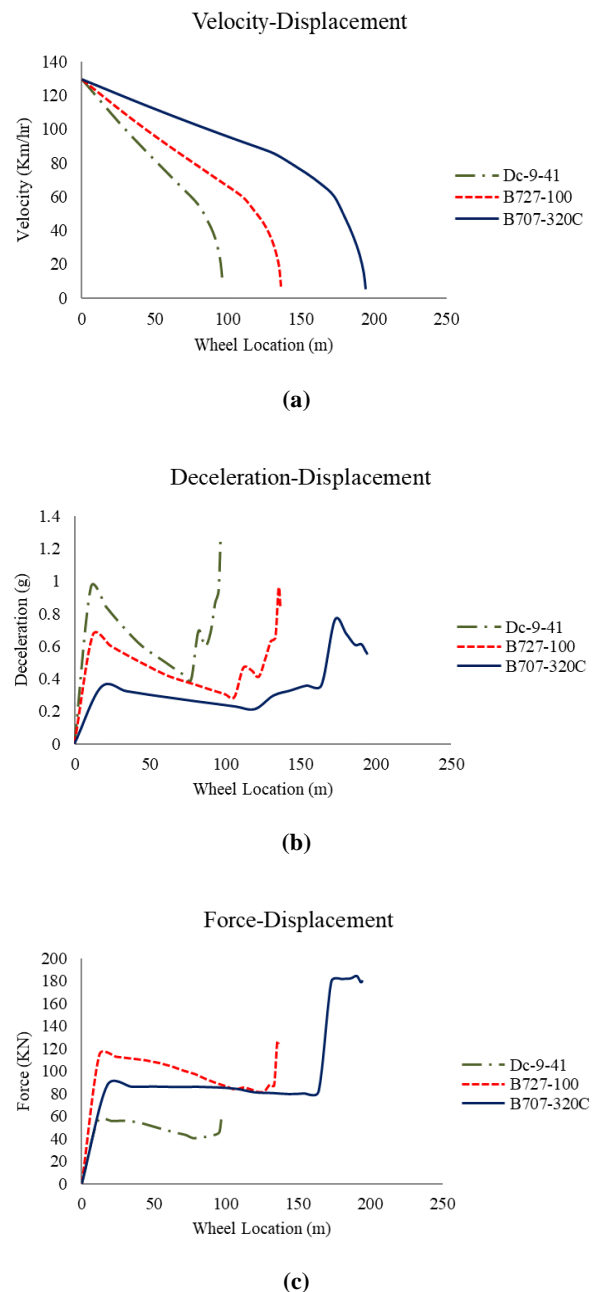


Fig. 7: a) Speed reduction, b) deceleration, and c) reaction force diagrams for three aircraft on foamed concrete FC1.

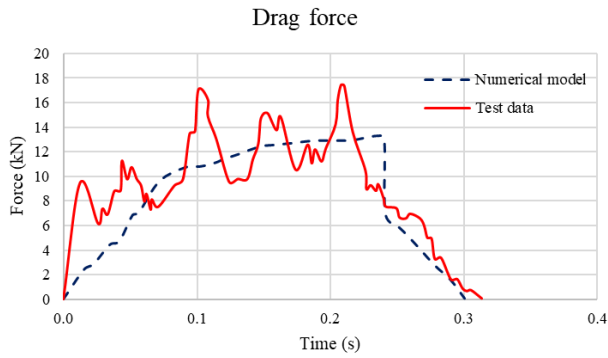


Fig. 5: Drag force comparison between numerical and experimental results.

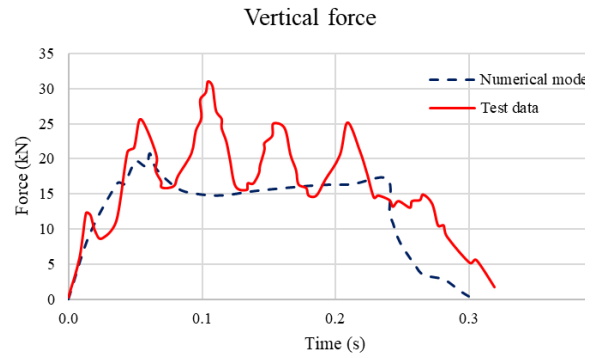


Fig. 6: Vertical force comparison between numerical and experimental results.

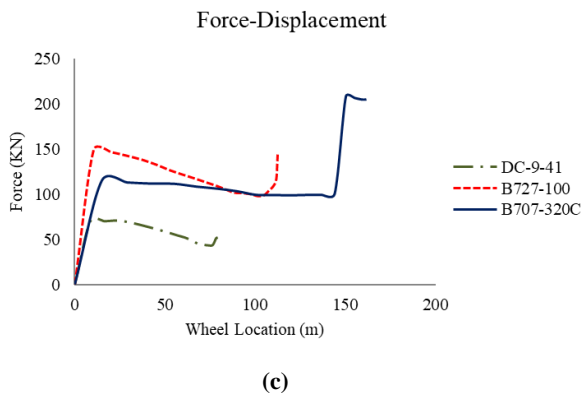
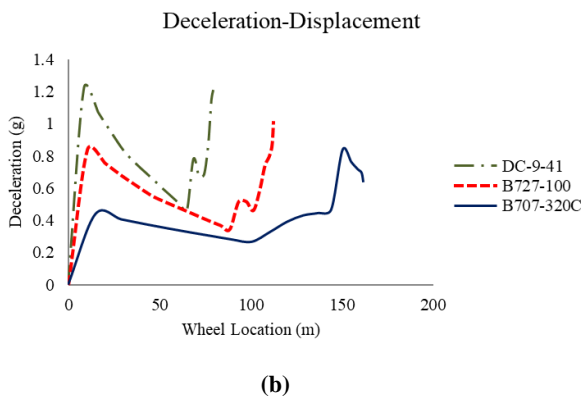
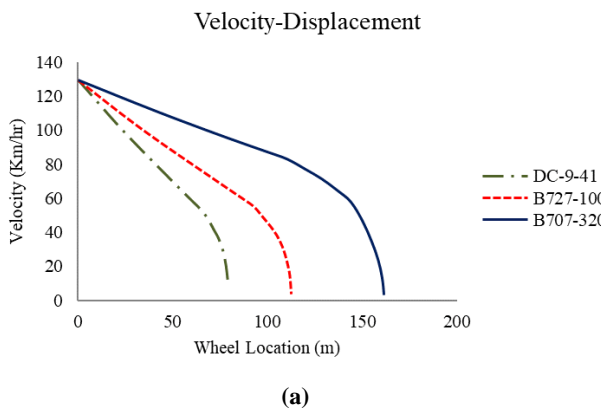


Fig. 8: a) Speed reduction, b) deceleration, and c) reaction force diagrams for three aircraft on foamed concrete FC2.

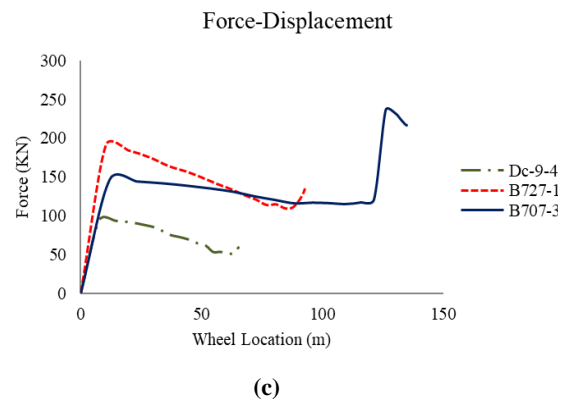
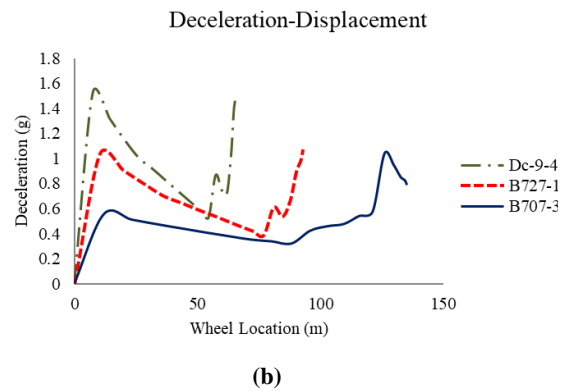
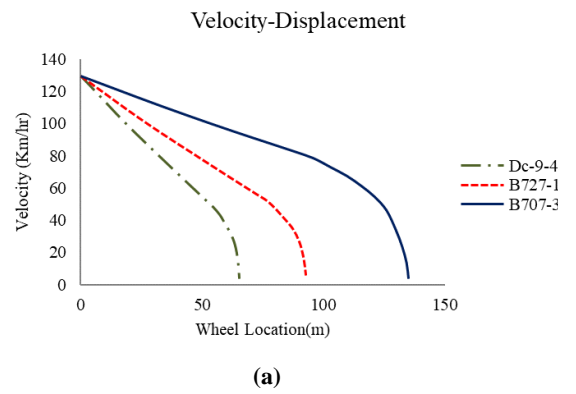


Fig. 9: a) Speed reduction, b) deceleration, and c) reaction force diagrams for three aircraft on foamed concrete FC3.

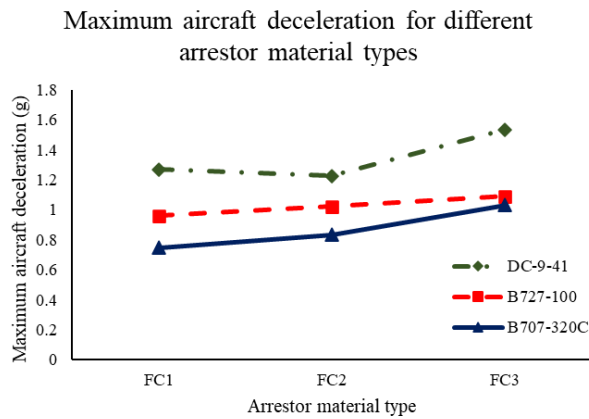


Fig. 10: Maximum aircraft deceleration for a different type of foamed concretes.

5. Conclusions

In this study, the ALE method for simulating the arrester bed under the loading of three different aircraft was investigated. In this modeling, a continuous bed with constant thickness is used. It is possible to use arrester beds with variable depths and shorter lengths, or even a bed with several materials (different properties) can be designed. Examining a combination of these conditions can also be helpful as new goals for studying EMAS.

The amount of stopping distance depends on several factors, such as the type of aircraft, the geometry of the bed, and the type of bed material. Naturally, the required length of the bed depends on the heaviest expected aircraft. Increasing the depth of the arrester bed and the compressive strength of the foamed concrete can reduce the stopping distance. However, this may lead to excessive loads on the aircraft wheels, which may cause damage in lighter aircraft such as the DC-9-41.

Acknowledgments

I would like to express my very great appreciation to Mr. Langary and Mr. Tahmasebi for their valuable suggestions and generous help in preparing this article.

References

- [1] R. E. David, "Location of commercial aircraft accidents/incidents relative to runways," Washington, DC, 1990.
- [2] I. Kirkland, R. E. Caves, M. Hirst, and D. E. Pitfield, "The normalisation of aircraft overrun accident data," *J. Air Transp. Manag.*, vol. 9, no. 6, pp. 333–341, 2003, doi: 10.1016/S0969-6997(03)00033-4.
- [3] J. Hall, M. Ayres, and D. Wong, *Analysis of Aircraft Overruns and Undershoots for Runway Safety Areas*. 2008.
- [4] F. A. A. FAA, "Engineered materials arresting system (EMAS) for aircraft overrun.," Washington, DC, 2005.

- [5] C. H. Ho and P. Romero, "Investigation of existing engineered material arresting system at three U.S. Airports," in *50th Annual Transportation Research Forum* 2009, 2009.

- [6] M. A. Barsotti, J. M. H. Puryear, and D. J. Stevens, *Developing Improved Civil Aircraft Arresting Systems*. 2009.

- [7] E. Santagata, M. Bassani, and E. Sacchi, "Performance of New Materials for Aircraft Arrestor Beds," no. 2177, pp. 124–131, 2010, doi: 10.3141/2177-15.

- [8] E. Heymsfield, W. M. Hale, and T. L. Halsey, "A Parametric Sensitivity Analysis of Soft Ground Arrestor Systems," *Aviation*. American Society of Civil Engineers, 2007, doi: 10.1061/40938(262)20.

- [9] E. Heymsfield, W. M. Hale, and T. L. Halsey, "Optimizing Low Density Concrete Behavior for Soft Ground Arrestor Systems," *Airfield and Highway Pavements*. American Society of Civil Engineers, 2008, doi: 10.1061/41005(329)11.

- [10] E. Heymsfield, "Predicting aircraft stopping distances within an EMAS," *J. Transp. Eng.*, vol. 139, no. 12, pp. 1184–1193, 2013, doi: 10.1061/(ASCE)TE.1943-5436.0000600.

- [11] Z. Q. Zhang, J. L. Yang, and Q. M. Li, "An analytical model of foamed concrete aircraft arresting system," *Int. J. Impact Eng.*, vol. 61, pp. 1–12, 2013, doi: 10.1016/j.ijimpeng.2013.05.006.

- [12] H. H. Zhao and H. Bin Yu, "Modeling and analysis of arresting property of EMAS," *Adv. Mater. Res.*, vol. 989–994, pp. 2829–2833, 2014, doi: 10.4028/www.scientific.net/AMR.989-994.2829.

- [13] Z. Q. Zhang and J. L. Yang, "Improving safety of runway overrun through foamed concrete aircraft arresting system: An experimental study," *Int. J. Crashworthiness*, vol. 20, no. 5, pp. 448–463, 2015, doi: 10.1080/13588265.2015.1033971.

- [14] X. Yang, J. Yang, Z. Zhang, J. Ma, Y. Sun, and H. Liu, "A review of civil aircraft arresting system for runway overruns," *Prog. Aerosp. Sci.*, vol. 102, no. July, pp. 99–121, 2018, doi: 10.1016/j.paerosci.2018.07.006.

- [15] N. Liu and H. Bin Yu, "The design of dynamic model of engineering material arresting system," *Appl. Mech. Mater.*, vol. 607, pp. 435–439, 2014, doi: 10.4028/www.scientific.net/AMM.607.435.

- [16] S. Researcher, H. Pavement, and S. Technician, "Design, Analysis, and Asphalt Material Characterization for Road and Airfield Pavements GSP 246 © ASCE 2014 170," pp. 170–177, 2014.

- [17] ATSB, *Runway Excursions Part 2: Minimising the Likelihood and Consequences of Runway Excursions*, vol. 018, no. 2. 2008.

- [18] P. K. Yadawa and R. R. Yadav, "Multidiscipline Modeling in Materials and Structures," *Multidiscip. Model. Mater. Struct.*, vol. 5, no. 1, pp. 59–76, 2009, doi: 10.1108/15736105200900004.

- [19] M. Nazem, J. P. Carter, and D. W. Airey, "Arbitrary Lagrangian-Eulerian method for dynamic analysis of geotechnical problems," *Comput. Geotech.*, vol. 36, no. 4, pp. 549–557, 2009, doi: 10.1016/j.compgeo.2008.11.001.

[20] C. W. Hirt, A. A. Amsden, and J. L. Cook, "An arbitrary Lagrangian-Eulerian computing method for all flow speeds," *J. Comput. Phys.*, 1974, doi: 10.1016/0021-9991(74)90051-5.

[21] M. Bakroon, R. Daryaei, D. Aubram, and F. Rackwitz, "Arbitrary Lagrangian-Eulerian Finite Element Formulations Applied to Geotechnical Problems," *Numer. Methods Geotech.*, vol. 41, no. September, pp. 33–44, 2017, doi: 978-3-936310-43-6.

[22] E. Heymsfield, W. M. Hale, and T. L. Halsey, "Aircraft response in an airfield arrestor system during an overrun," *J. Transp. Eng.*, vol. 138, no. 3, pp. 284–292, 2012, doi: 10.1061/(ASCE)TE.1943-5436.0000331.



This article is an open-access article distributed under the terms and conditions of the Creative Commons Attribution (CC-BY) license.